63-3-2

(5) 943 100

# PHOTOELECTRIC INFORMATION STORAGE

Interim Report No. 2

Contract No AF33(657)8715

For the Period

1 September 1962 to 30 November 1962

W. G. Reininger
A. S. Jensen
W. G. Beran

WESTINGHOUSE ELECTRIC CORPORATION
Electronic Tube Division
Baltimore, Maryland



$3.60

A51035ARID
437B

# PHOTOELECTRIC INFORMATION STORAGE.

Interim Report No. 2,

Contract No. AF33(657)8715

N/A

For the Period

1 September 1962 - 30 November 1962,

by W. G. Reininger,
A. S. Jensen and
W. G. Beran.

30 Nov 62, iv, [illegible] tables, 8 refs.

WESTINGHOUSE ELECTRIC CORPORATION
Electronic Tube Division
Baltimore, Maryland

## ABSTRACT

Additional experiments with the electronic shutter showed no leakage of photoelectrons.

It was found that the surface roughness of the nickel electroformed targets was resolved with the WX-4787 high resolution reading gun. Several cleaning techniques were tried to improve the surface characteristics. The final solution of this problem will probably be found in a blemish-free master.

A feasibility study was made of electron beam exposure of a photographic emulsion for TVIST recording. The entire experiment was performed with existing TVIST equipment. The recorded resolution was 2100 TV lines per inch, but the limit is probably much higher. This process can be used in place of or in addition to the kinescope and camera of the slow scan recording unit.

Problems with discontinuities of the spiral accelerators were solved by redesigning the masking tool. Several spiral envelopes were produced with an isolated photocathode to permit better processing control.

Preliminary target electroforming experiments were performed on a small plating bath with excellent results. A large bath was set up and is now in operation.

A more elaborate study of the noncharging, nondestructive readout was started. It is hoped that this study will result in increased sensitivity. Also, measurements were made to determine return beam modulation as a function of dielectric and target base potentials.

The experimental work for the construction of the 4.5-inch deflection system has been completed, and the construction of the chassis is well under way.

A new deflection chassis for the 3-inch flip-over tube test rack was built.

The slow scan test rack has been moved to the tube laboratory for use with the flip-over target tubes. Interference from 60 cps power is still a problem.

The addition of a sixth multiplier stage to the standard return beam structure improved the overall gain by a factor of two or three.

Three spiral test tubes for determining the activity of bialkali photocathodes were assembled and processed. The spectral responses of two S-20 and one bialkali photosurfaces were measured.

Two 3-inch spiral photodiodes are being evaluated for resolution and distortion. The highest center resolution was found to be 3400 TV lines per inch.

Electrostatic Latent Image Development (ELID) principles were applied to the TVIST system to see if the contrast of a decayed image could be improved significantly. Contrast gains of about 20 times were shown. This process can be repeated several times.

Existing data on dielectric constants and specific resistances are included as an appendix. These data concern various alkali and alkaline-earth halides and oxides which are suitable for vacuum evaporation, thin film studies.

# TABLE OF CONTENTS

## 1. INTRODUCTION



## 2. FACTUAL DATA



## 3. PROGRAM FOR NEXT INTERVAL



## APPENDIX A. STUDY OF DIELECTRICS

## BIBLIOGRAPHY



## LIST OF ILLUSTRATIONS

# 1. INTRODUCTION

The experimental determination of the design parameters of the Tape Camera Storage Tube is continuing. This effort, which was begun on contract No. AF33(616)6666, is continuing on contract No. AF33(657(8715. The device will be capable of taking pictures in visible light by means of a photoemissive surface, store many of these pictures as an electric charge pattern on a dielectric on a metal base tape, read this information out on command, as a video signal at a very high data rate, erase the unwanted information on command, and reuse the storage tape a great many times.

# 2. FACTUAL DATA

This section outlines the accomplishments made during the reporting period. For convenience of discussion, work progress is divided into the following topics: demountable system, spiral accelerators, target tape, electronic equipment, vacuum tube development and electrostatic latent image development. The following paragraphs discuss these topics.

## 2.1 DEMOUNTABLE VACUUM SYSTEM

### 2.1.1 Electronic Shutter

Some additional experiments with the electronic shutter showed that there is no leakage of photoelectrons through the shutter mesh. A 5-minute exposure to high voltage with the shutter closed made no visible difference in charge on the target. The functioning of the shutter was demonstrated by replacing the target with a phosphor. No time lag and no leakage could be observed.

### 2.1.2 Target Evaluation and Cleaning

The WX-4787 high resolution reading gun was installed on the ultraviolet demountable vacuum system. This gun, along with a 500-mesh photocathode pattern, was used to evaluate the surfaces of nickel targets and, thus, to determine the effectiveness of different cleaning techniques. The high resolution gun resolved the crystallinity of the nickel surface much more sharply than the standard orthicon gun which had been used for several months.

A series of tests was made on targets which were hydrogen fired at different temperatures. Some improvement was noticed with low temperature firing, but a certain granularity was still evident. An improved cleaning technique using acetic acid was also tried, with promising results. However, most of the surface irregularities probably will not be eliminated until a very clean blemish-free master is made from the diffraction grating replica.

### 2.1.3 Photographic Electron Recording

A study made during the last work period determined the practicability of electron exposure of a photographic emulsion for TVIST recording. Experiments were made to determine roughly the problems which could be encountered with such a technique.

Additional experiments, using the equipment and parts available in the laboratory, were made to determine a resolution limit.

The demountable vacuum system which has been used for testing targets was set up with the eight position target holder and a 5CE high resolution cathode ray gun. This gun had been used for earlier TVIST storage experiments. Special glass negative plates designed for electron microscope use were obtained. These plates have a medium high contrast emulsion especially suited for electron exposure. A 10-kv accelerating potential was used on the writing gun beam, and the video signal was derived from a stored picture on the TVIST flip-over target tube. The beam scanned the emulsion with a regular TV raster, the height of which was 0.5 inch.

After exposure the plates were developed for 6-minutes in a high contrast developer. Then they were fixed, washed, and dried. The best exposures were picked by microscopic examination, and 10X enlargements were made of them on high contrast paper. The raster height on the plates was measured to be 0.5 inch. The photograph (figure 1) shows one of these enlargements. Microscopic examination of this picture shows about 100 scan lines per inch, indicating that a full 525-line raster was present. Thus, a resolution of about 2100 TV lines per inch was recorded on the plate. It is obvious from the width and sharpness of the scan lines, and the fact that the interlace is slightly paired, that even higher resolution can be obtained quite easily. Some of the spots on the picture are on the storage targets of the flip-over tube, and others were dust on the photographic plate. This system can be used for a high resolution recording of stored information.

## 2.2 SPIRAL ACCELERATORS

During this period, resistance interruptions on evaporated thin film spirals caused some difficulty. Intensive investigation indicated that ridges and irregularities on the inside of the glass envelope caused the masking tool to chatter. A new tool having no play and incorporating several new advantages was designed, built and tested. Subsequent microscopic investigation of evaporated spirals showed that the new tool removed the mask material without chatter. However, some difficulty is still encountered when pronounced ridges are present on the inside of the glass envelope. Thus it is possible that precision ground glass tubing will be necessary for future spiral envelopes.

Several spirals were produced for 3-inch and 4.5-inch photodiode flip target tubes. The 4.5-inch envelopes included a separate button near the front of the tube envelope

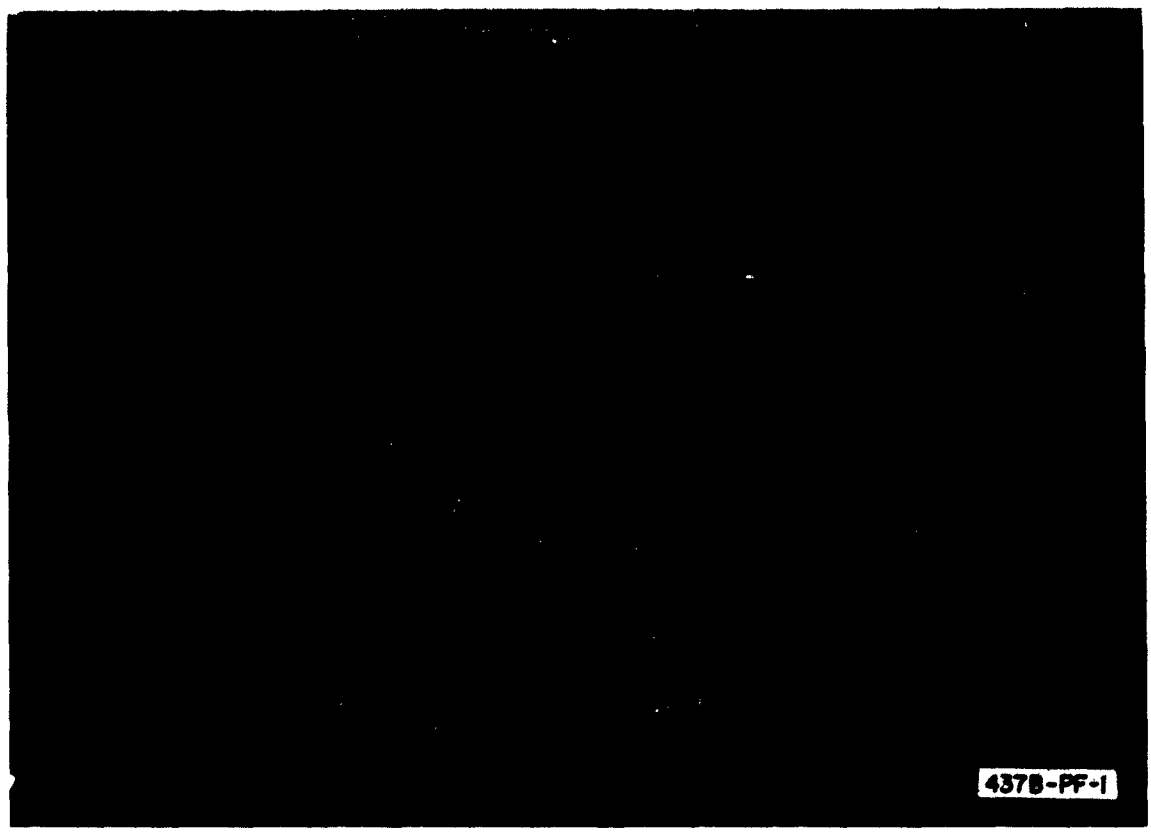


Figure 1. Electron Writing on Photographic Emulsion

so that the spiral could be electrically isolated from the photocathode during photocathode processing. This technique eliminates leakage currents which mask photocathode response and permits a direct measurement of photocathode current. This measurement is particularly important for good control during processing.

During recent tube fabrication, some difficulty has been encountered because of mechanical fragility and resistance changes in the evaporated thin film spirals during bakeout. Past experience has shown that, if proper cleaning and evaporation techniques are followed, these evaporated spirals should be mechanically and electrically stable. This problem will be solved by careful analysis and standardization of techniques.

## 2.3 TARGET TAPE

### 2.3.1 Target Electroforming

Preliminary target electroforming experiments were run on a small bath with excellent results. Several pieces were electroformed from both nickel and aluminum masters. These pieces were made in thicknesses from 0.0008 inch to 0.30 inch. The pieces produced in this way exhibited excellent springiness and the physical properties necessary for use as storage tape. No difficulty was observed in plating or stripping from plastic and metal substrates.

A large 3-gallon nickel electroforming bath was set up for target electroforming and is in operation. This bath is a special low stress nickel sulfamate. The tank has a regulated power supply, an immersion heater, and an automatic water refill to keep the bath level constant during long plating times. A mechanical stirring device keeps the bath temperature evenly distributed. The tank has been installed in a hood to permit cleaner work and the removal of gas products which may be evolved during plating.

A high quality diffraction grating was installed in a plastic frame and evaporated with a conductive coating of silver. The piece is presently being electroformed to a thickness of 0.050 inch to maintain rigidity and to serve later as a master for electroforming copies of it.

### 2.3.2 Target Electric Field Analysis

A more elaborate study of the noncharging, nondestructive readout was started. With this analysis, it is hoped that further increases in sensitivity will result. Figures 2 through 7 show Teledeltos electric field plots with electron trajectories. For all the plots it was assumed that the target dielectric had been primed to -16 volts with respect to the metal base and the reading cathode gun was held at -11 volts with respect to the target base. Figures 2 through 7 have the uniform target prime charge decreased by the writing process from -16 volts to -15, -14, -13, -12, and -11 volts respectively. It is shown on the figures that the return beam is changed by the different charges from 100 percent to 6.3 percent (or modulated from 0 to 93.7 percent).

Also, measurements were made to determine the return-beam modulation as a function of the potential on the dielectric surface with respect to the cathode ($e_{kd}$) and of the potential on the target base with respect to the cathode ($e_{kt}$). For noncharging reading (nondestructive reading), a varying portion of the primary reading beam is collected by the bare slopes of the target grooves. This portion of the

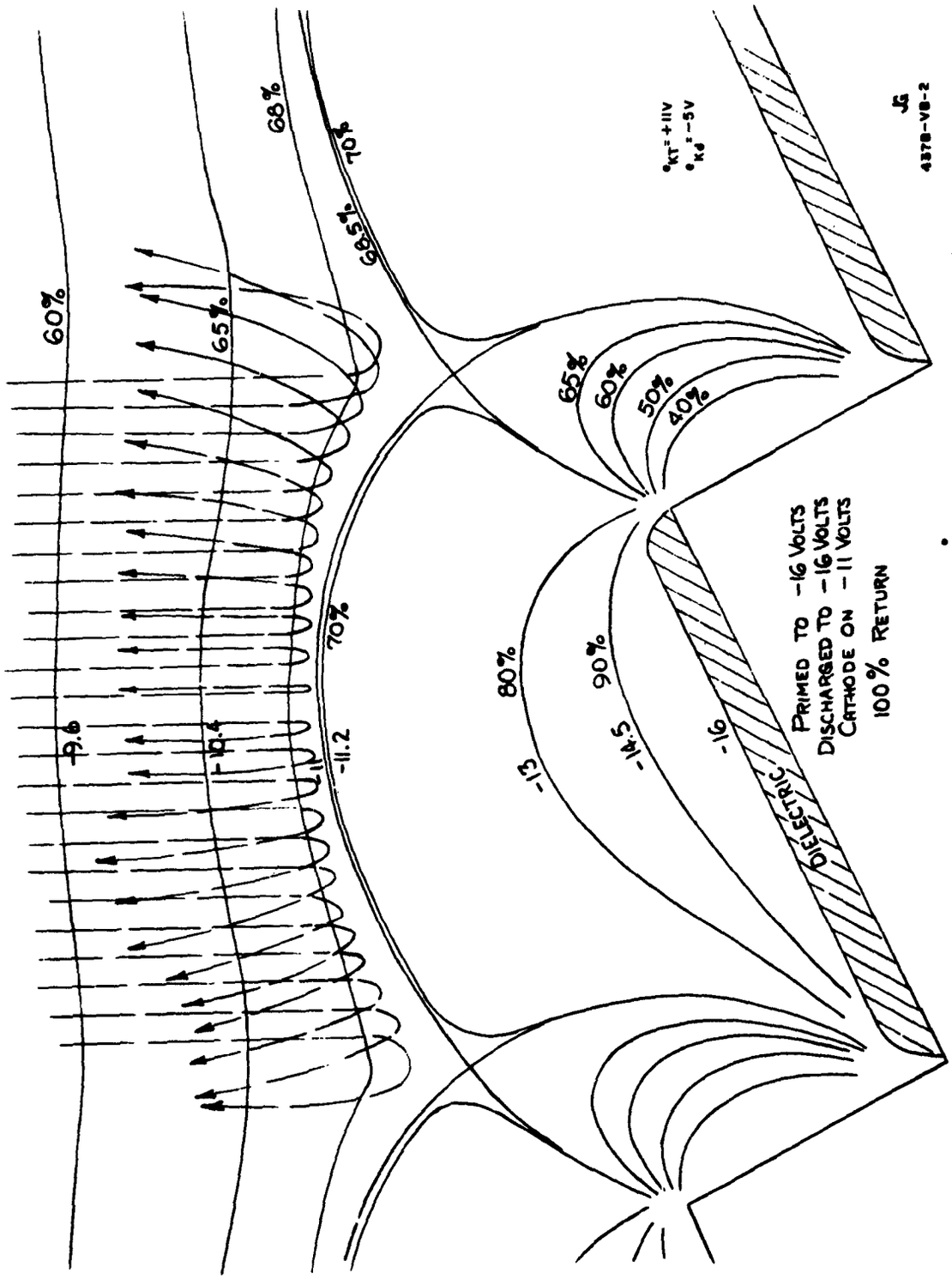


Figure 2. Teledeltos Electric Field Plot Showing Electron Trajectories

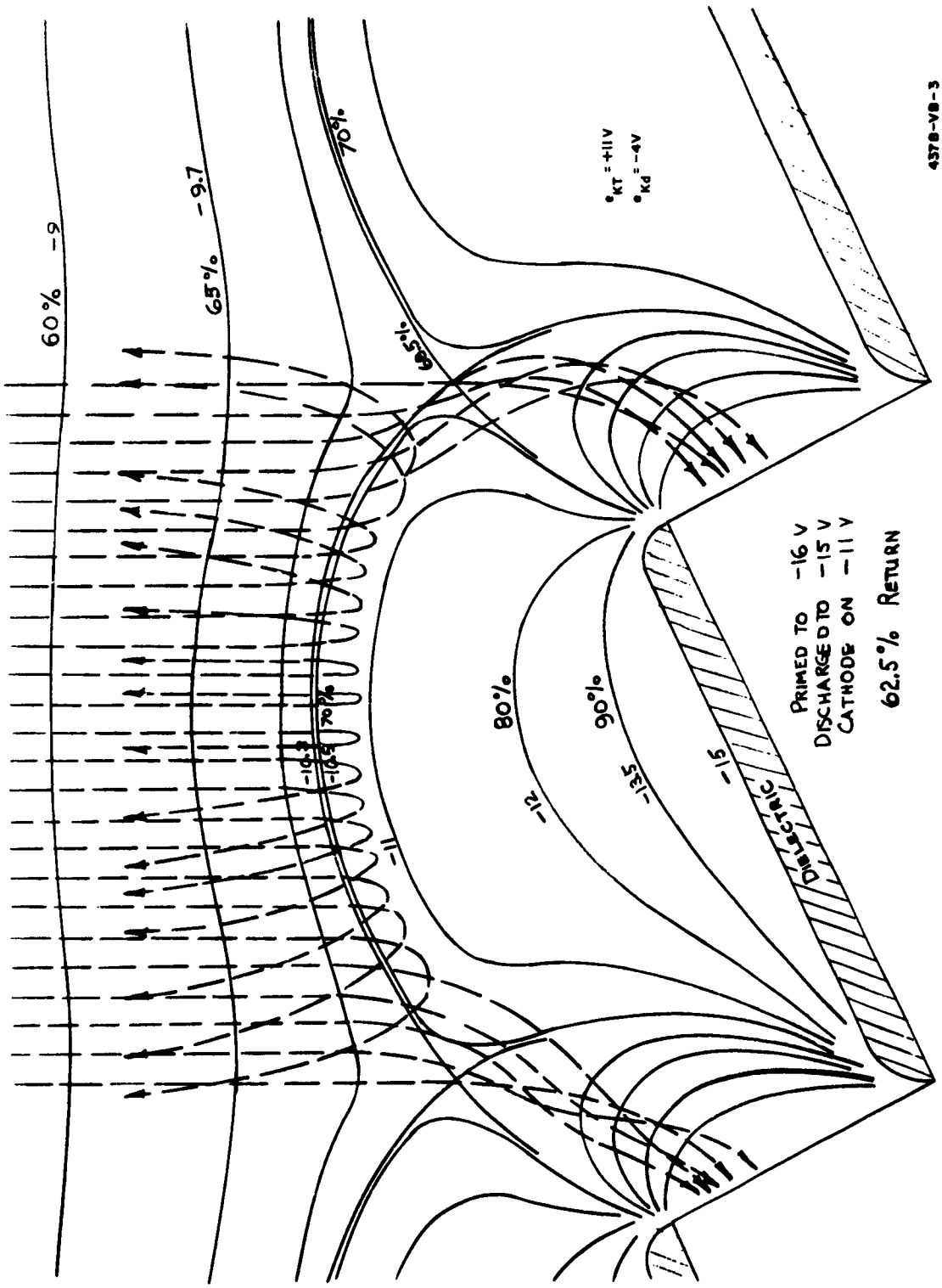


Figure 3. Teledeltos Electric Field Plot Showing Electron Trajectories

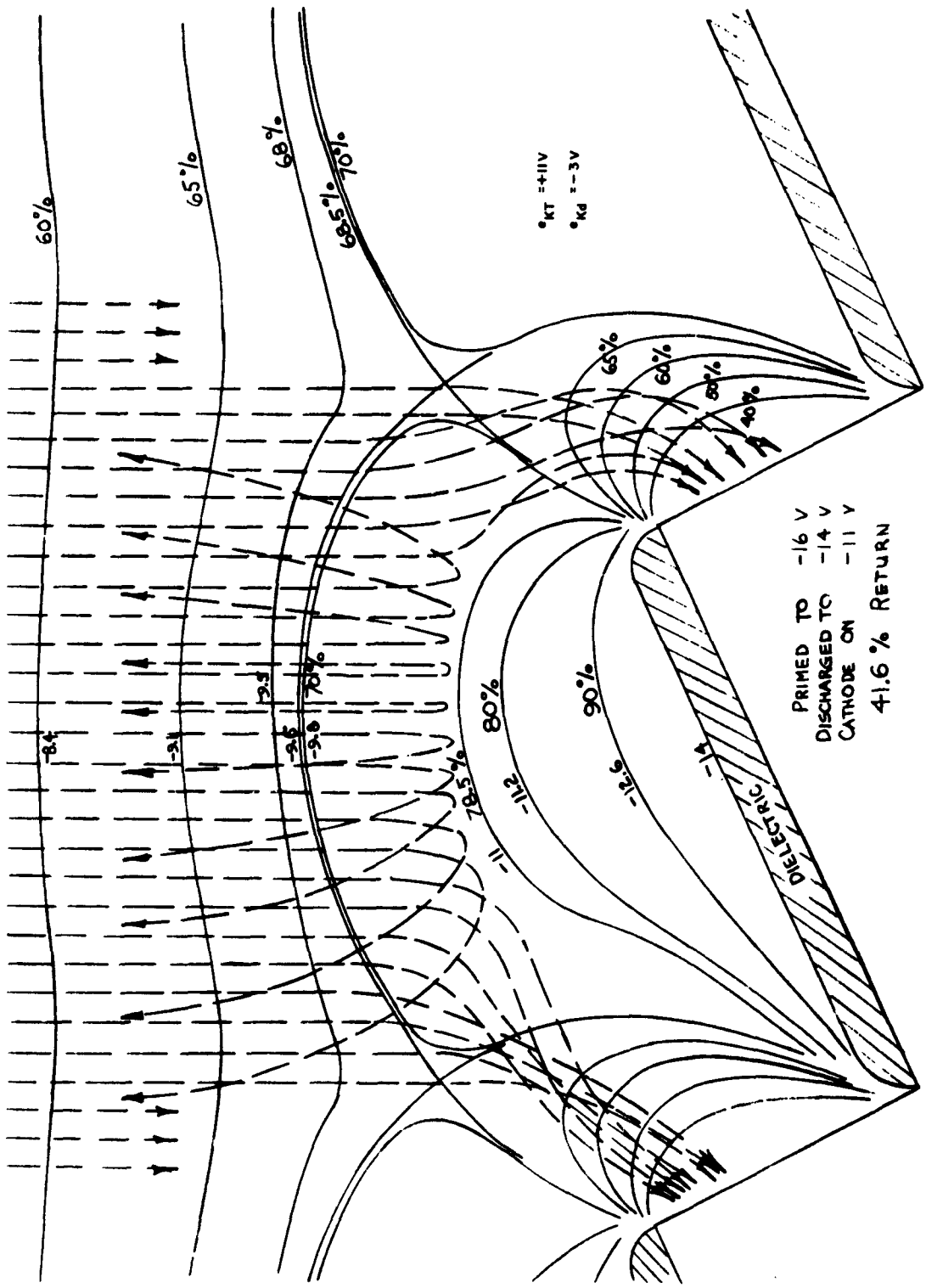


Figure 4. Teledeltos Electric Field Plot Showing Electron Trajectories

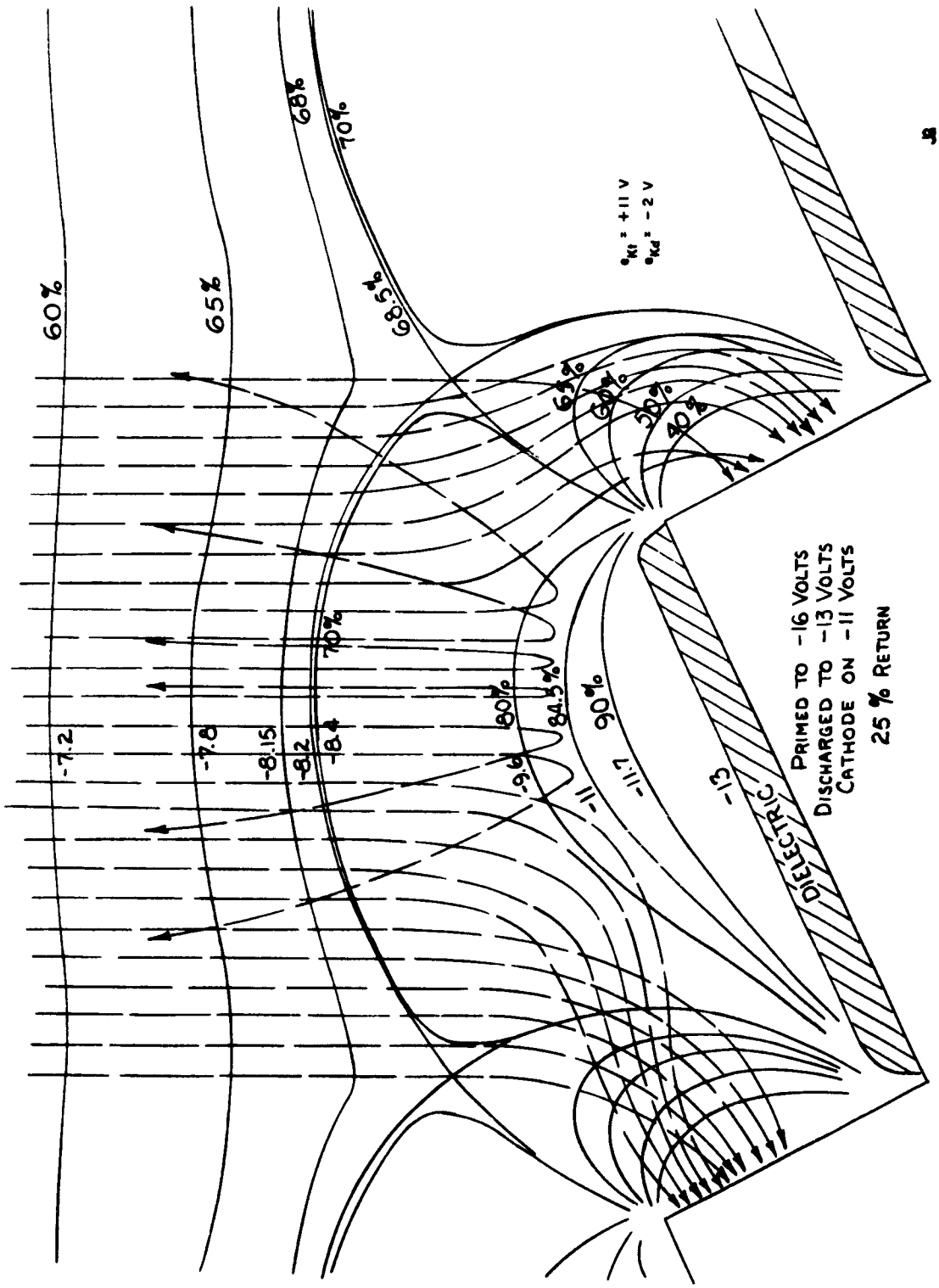


Figure 5. Teledeltos Electric Field Plot Showing Electron Trajectories

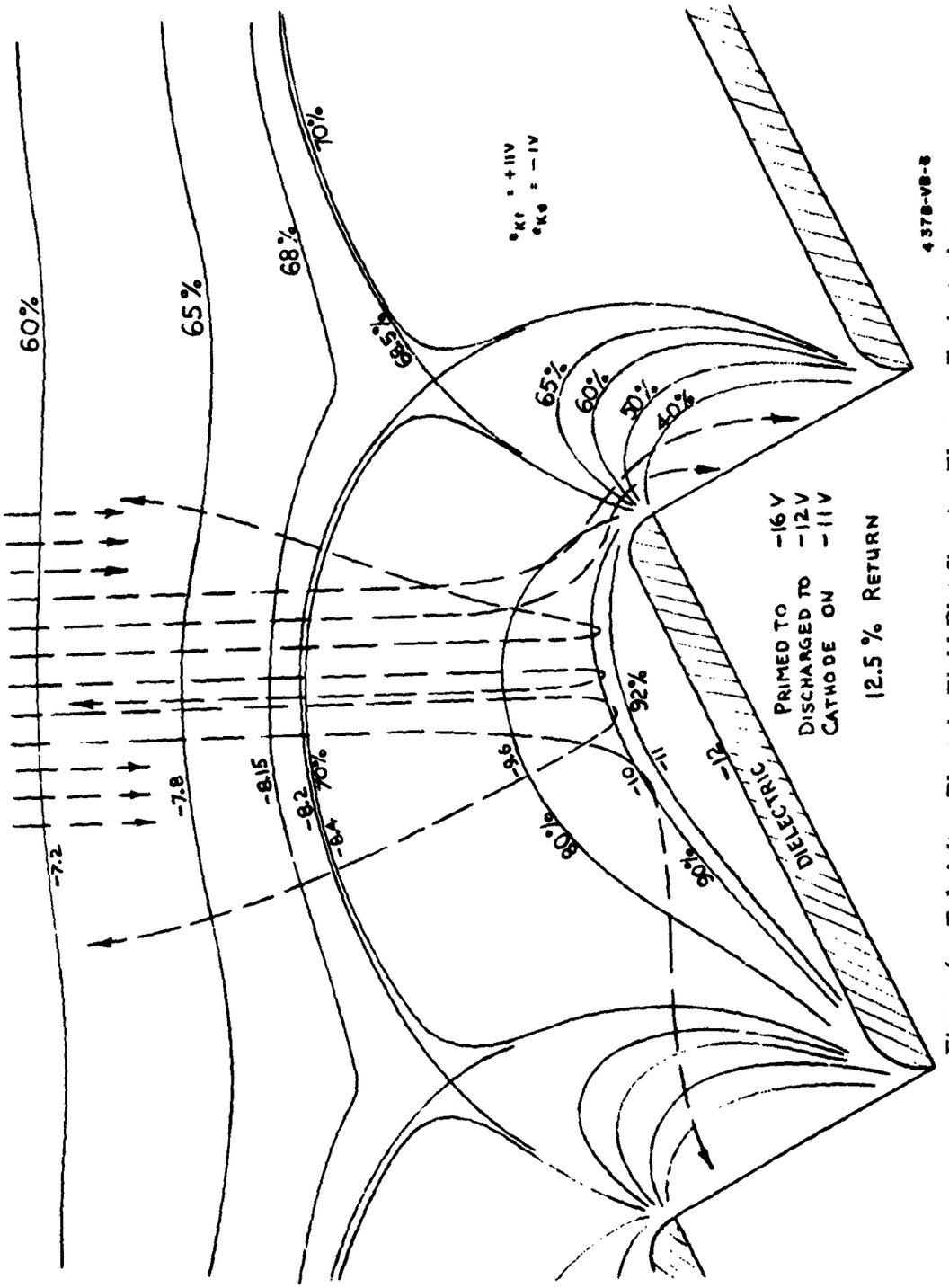


Figure 6. Teledeltos Electric Field Plot Showing Electron Trajectories

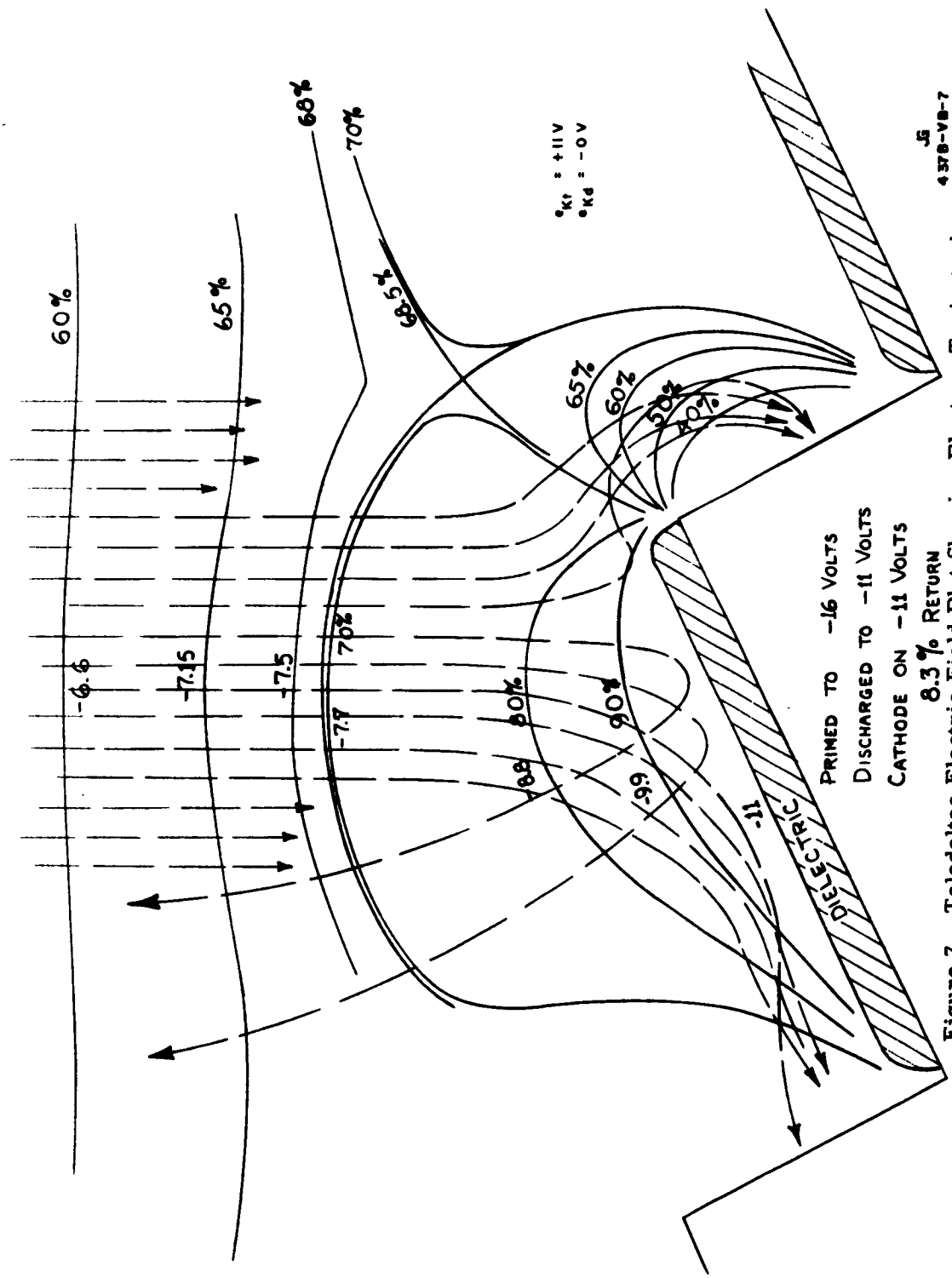


Figure 7. Teledeltos Electric Field Plot Showing Electron Trajectories

primary beam depends on $e_{kd}$ and $e_{kt}$ and constitutes the modulation of the return beam.

The measurements for figure 8 were made with a constant primary beam of 50 x $10^{-9}$ ampere. The curve for $e_{kt}$ = +11 volts is commonly used for readout in our storage experiments. The dielectric surface had been primed to -16 volts with respect to the target base and an electrostatic pattern was produced by writing (discharging) part of this surface charge. For reading, the cathode is now set to -11 volts with respect to target base ($e_{kt}$ = +11 volts).

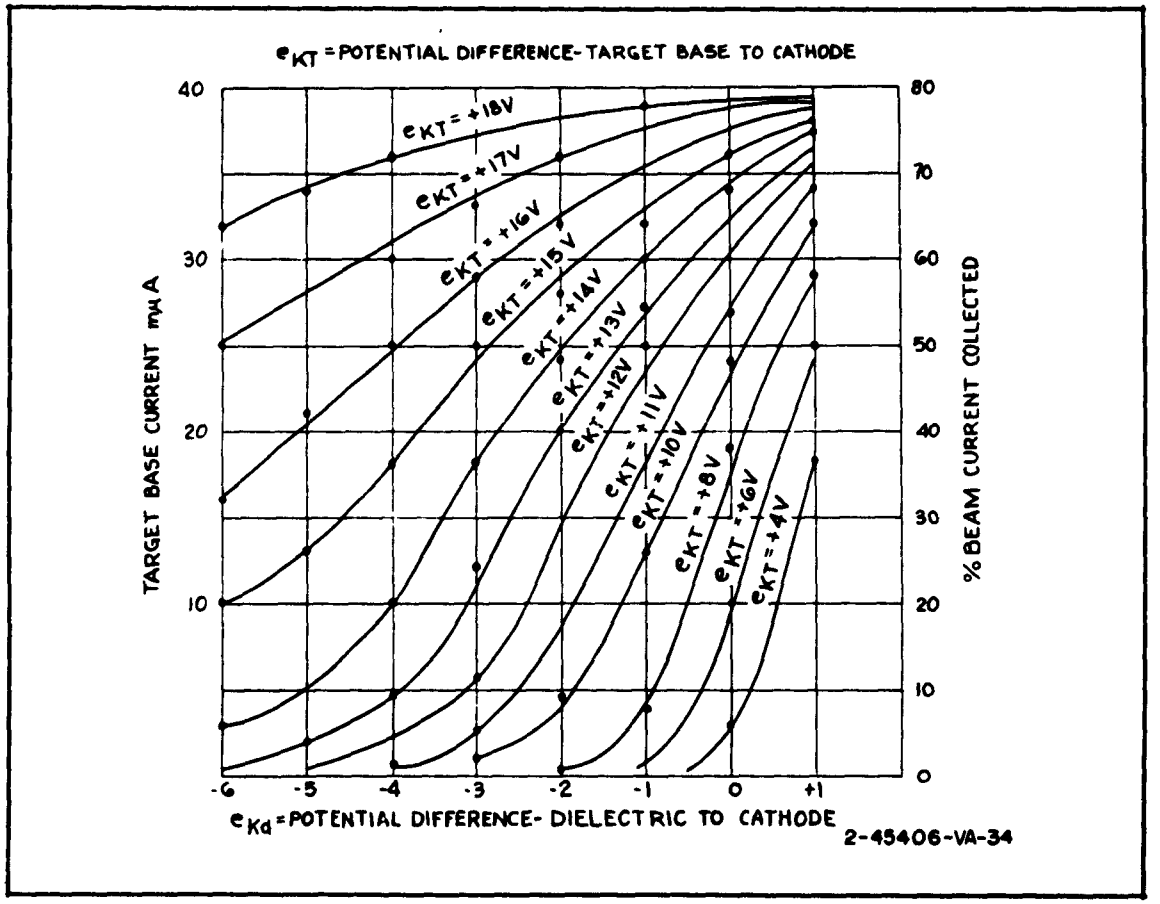


Figure 8. Transfer Curves; Primary Beam Constant at 50 x $10^{-9}$ Ampere

For a linear transfer, only the straight part of the curve $e_{kt}$ = +11 volts is used. For nondestructive readout this curve can be used only to where $e_{kd}$ = 0. (Points further to the right on this curve will have electrons landing during readout. These

electrons will produce a change in the stored pattern.) The writing (exposure) is continued to the point where the potential pattern on the dielectric is from -3 volts to 0 volt, but only with respect to the reading cathode. This potential range on the dielectric surface modulates the return beam more than 60 percent. Figure 2 to 7 show return beam modulation for the previous parameters which were derived from Teledeltos plots by using Snell's law.

In figure 9 the transfer curve found by Teledeltos plot is shown broken, and the corresponding curve from figure 8 is shown solid. The large disagreement between the curves seems to be due to contact potentials of the cathode and the bare metal parts of the target and also to slight variations in the geometry of the assumed target shape. Further analysis will be done to correlate the results.

## 2.4 ELECTRONIC EQUIPMENT

The experimental work for the 4.5-inch image orthicon deflection system has been completed. A circuit has been designed which will drive the deflection coils with up to 2 amperes peak to peak on the horizontal and 400 milliamperes on the vertical. It was necessary to design a special horizontal output transformer to permit over-scanning. The construction of the deflection chassis is well under way and the focus current supply has been completed. The rest of the necessary equipment is already in existence for the operation of the 4.5-inch flip target tube.

A new deflection chassis for the existing 3-inch flip target tube test rack was constructed. This chassis incorporates several new features which permit a wider range of scan size adjustment and better control of linearity.

The slow scan test rack has been moved to the tube laboratory for use with flip target tubes. Some further electronic development still needs to be done, however.

Some difficulty has been observed with 60-cps interference and random vertical grouping of horizontal lines. It has been determined that part of the 60-cps problem is caused by alternating current interference from the tube heaters. The other part of the ac interference originates with the 60-cps room illumination. This interference is introduced into the video circuits.

In the past, the transistor vertical driver circuits drew too much current because of zener diode overheating. This difficulty has been corrected.

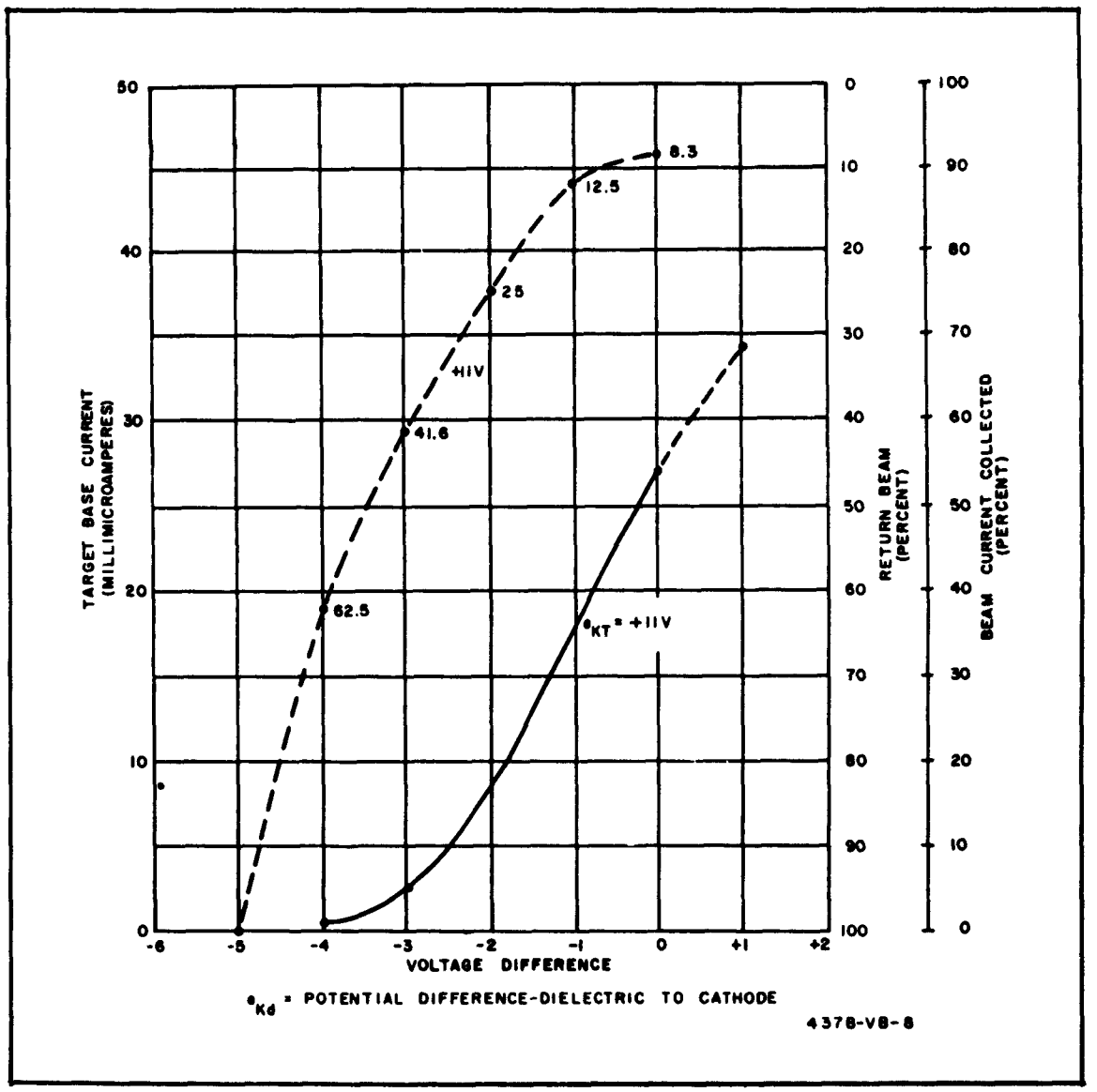


Figure 9. Transfer Curves

## 2.5 VACUUM TUBE DEVELOPMENT

### 2.5.1 Tube Fabrication

One flip target tube produced during this period had six multiplier stages instead of five as in the normal image orthicon and the previous flip target tubes. With six active stages on the tube, the gain was 2 to 3 times higher than normal, with no increase in noise. The beam current could thus be decreased to about one-half of normal by biasing grid No. 1 more negatively. The picture quality remained good. Reducing the beam current should reduce the focal spot size, and will be tried on a slit target tube. In the future, all flip target tubes, including the 4.5-inch tubes, will include a sixth multiplier stage.

Two 3-inch flip-over target tubes were processed with spiral accelerators. The pre-evaporated antimony substrate on the photocathode was accidentally removed during glow discharge cleaning, resulting in no photo response. An improved cleaning schedule is being developed.

Two 3-inch spiral photodiode tubes were completed during this period using an improved photosurface cleaning procedure.

### 2.5.2 Beam Size and Photocathode Research

Three spiral test tubes for determining the activity of bialkali photocathodes were assembled and processed. One tube produced 60 microamperes per lumen, the second produced 61 microamperes per lumen, and the third produced 80 microamperes per lumen. These tubes had the activation channels in the normal geometrical configuration, with only the material fill in the channels changed slightly from tube to tube.

The spectral response characteristics of two S-20 and one bialkali photosurface were measured with a calibrated monochromator. The response was plotted in milliamperes per watt versus wavelength in microns, as shown in figures 10, and 11, and 12. The S-20 photosurfaces have a response which extends somewhat farther into the red than the bialkali (figure 11).

### 2.5.3 Photodiode Resolution

Two 3-inch spiral photodiodes are presently being evaluated for distortion and resolution. The highest center resolution measured is 3400 TV lines per inch. Further measurements on the falloff in resolution away from the center are in progress, and photographs will be made.

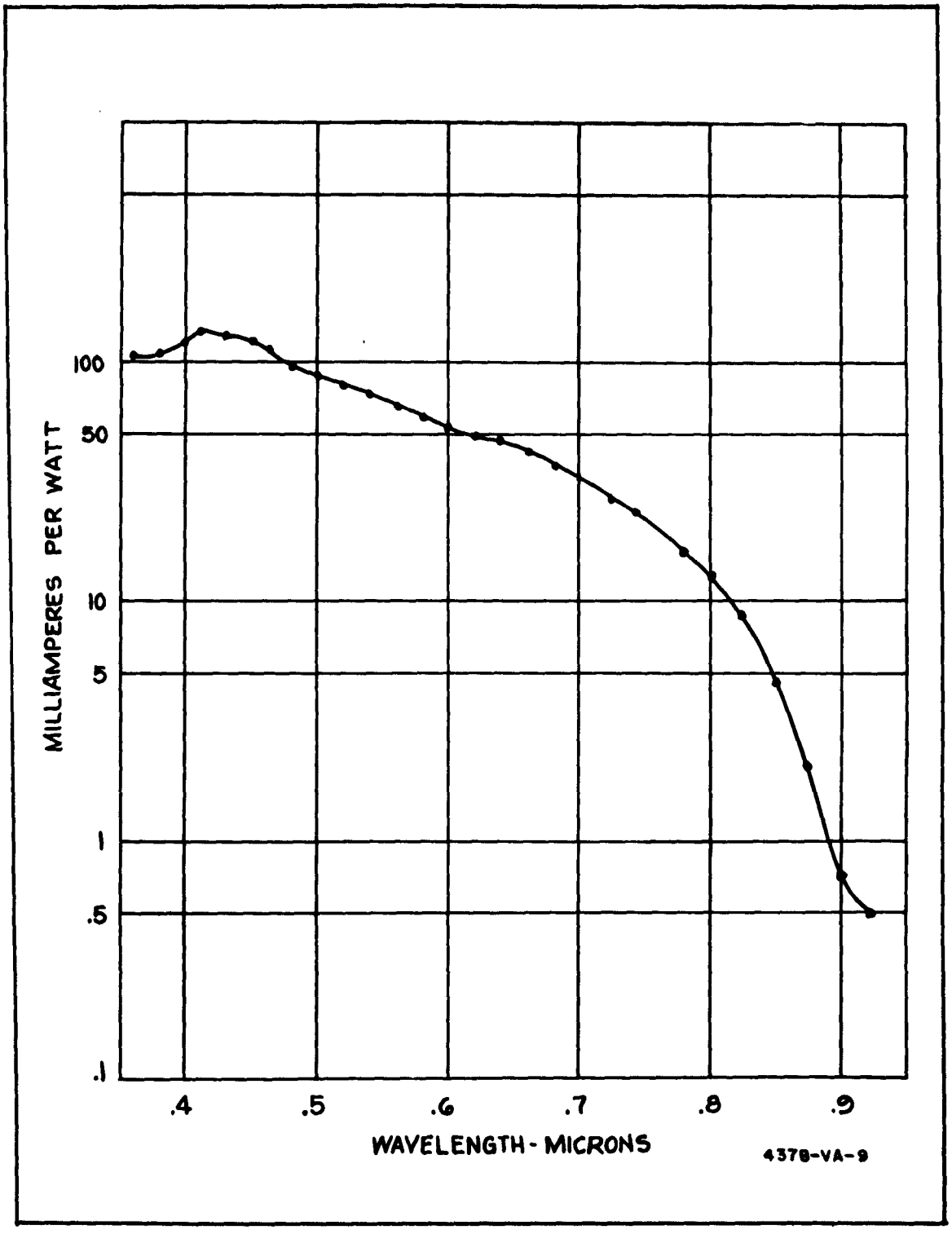


Figure 10. Spectral Response Characteristics

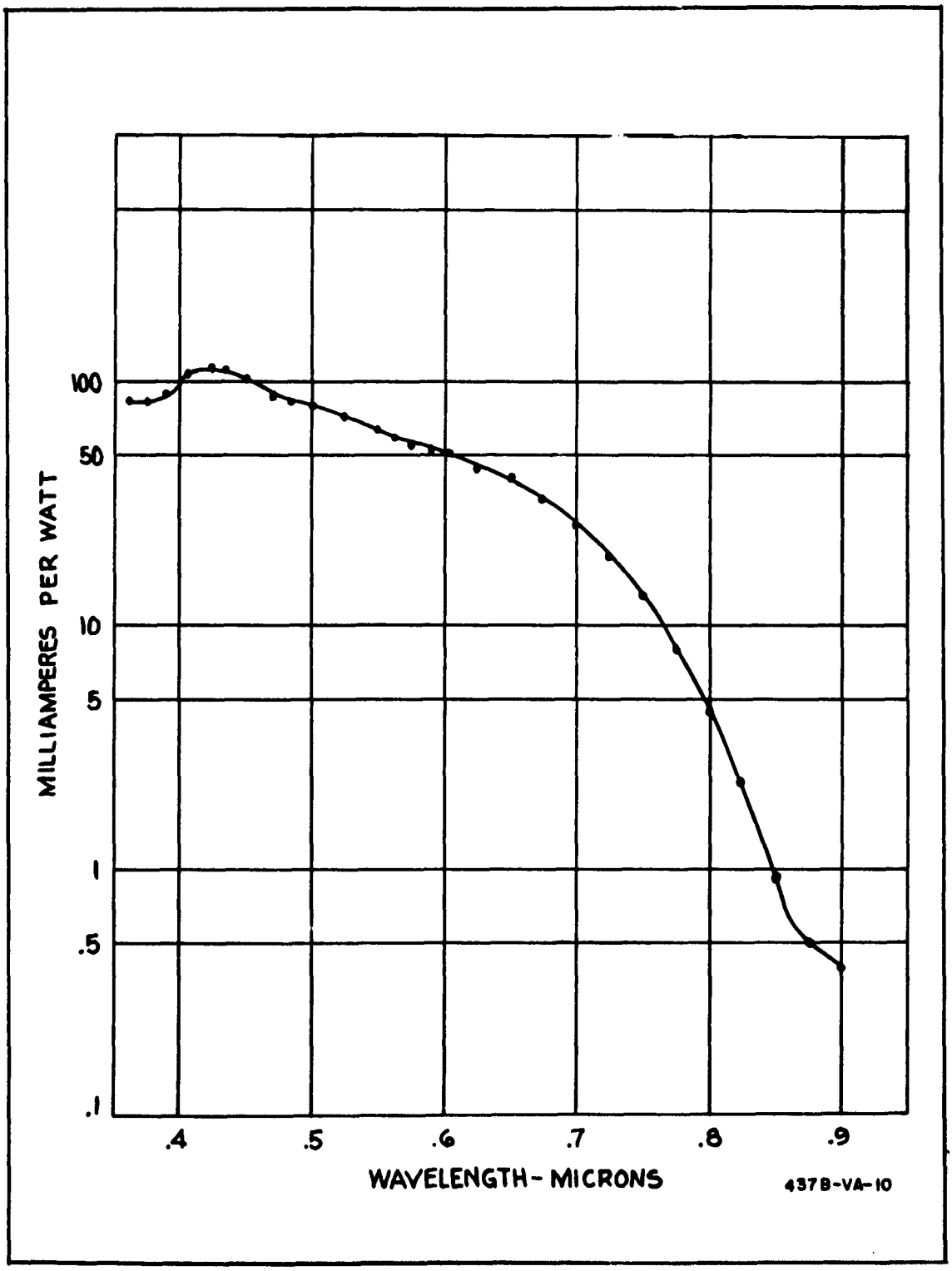


Figure 11. Spectral Response Characteristics

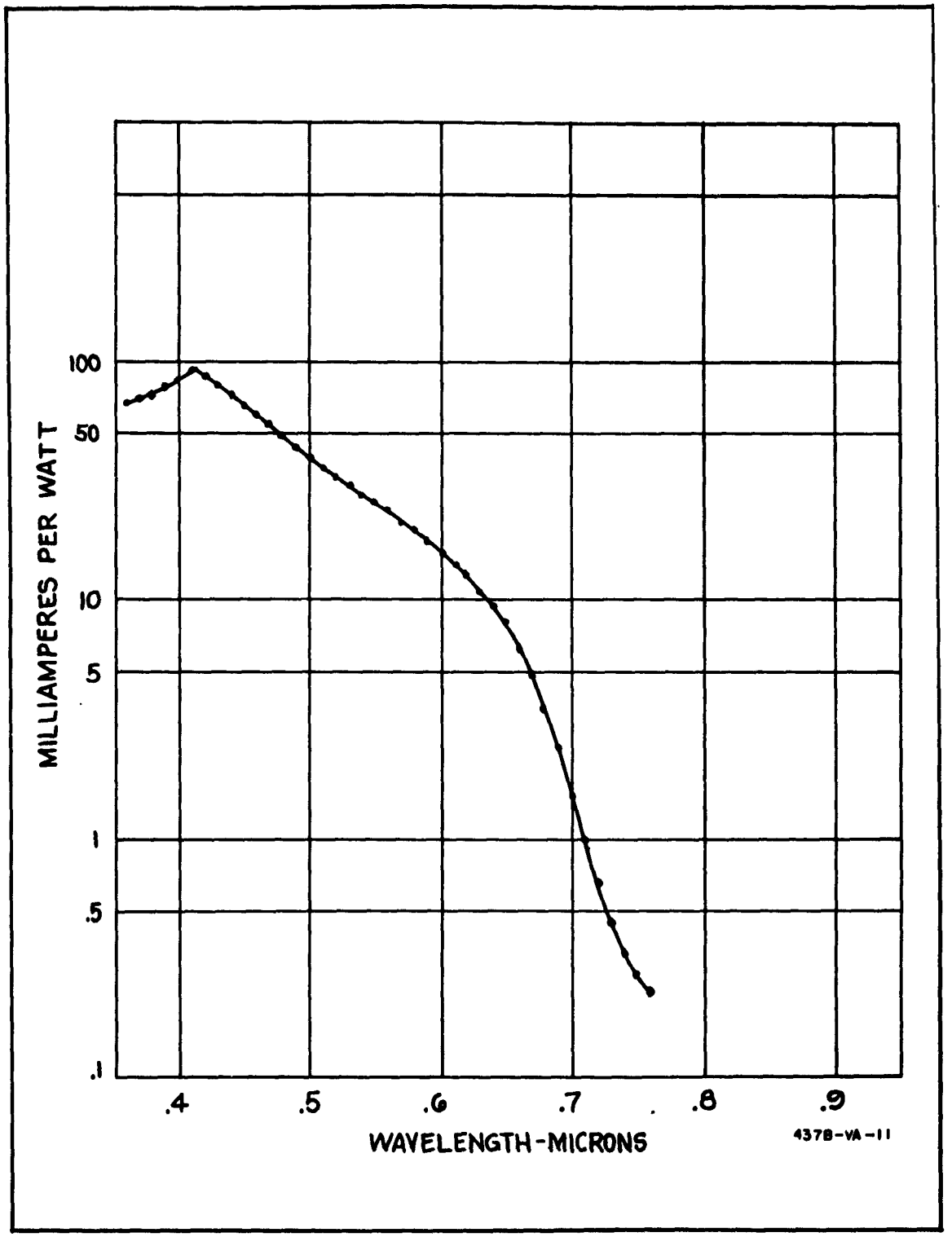


Figure 12. Spectral Response Characteristics

A new setup is being designed and built to permit operating the photodiode resolution setup on an optical bench. Because the maximum resolution of the lens system is on the optical axis, the setup will permit the photocathode to be moved from side to side. In this way the maximum resolution of the lens system can be used for measurements across the entire photocathode surface.

The Westinghouse Diminishing Line Resolution Pattern will be used to determine the ultimate limiting resolution of the photodiode without measuring directly on the phosphor. Photographs of the image on the phosphor will be made and subsequently scanned by a microdensitometer to determine the resolution characteristics.

## 2.6 ELECTROSTATIC LATENT IMAGE DEVELOPMENT

Under normal working conditions in a TVIST tube, the target surface is charged to a uniform potential of about -16 volts (see paragraph 2.3.2). Information is stored on the target by differentially discharging this prime charge. For optimum readout, a potential spread of -14 to -11 volts (on the dielectric with respect to the target base) results in a 60-percent modulation of the return beam for nondestructive readout, provided the cathode is at -11 volts with respect to the target substrate (see figure 9). However, after a long storage time or a long readout, the differential charge pattern will decay because of leakage or positive ion landing. Writing with a signal derived from such a differential charge pattern will result in a readout signal which is barely above the reading beam noise.

In these experiments, Electrostatic Latent Image Development (ELID)* re[illegible] electrostatic storage patterns whose potential spread on the target had deter[illegible] for example, to 0.5 to 0.7 volt. Repeated experiments showed that ELID successi[illegible] multiplied all of the target potentials by a factor of 20, resulting in a potential spread of 10 to 14 volts. A reading gun cathode at -10 volts with respect to the target base produced a fully readable signal. Before ELID, there was little or no signal.

A bar pattern had been stored on the dielectric of a TVIST tube. The surface was scanned with a reading beam and the return beam was modulated by the stored charge pattern. The output of one horizontal line is shown in figure 13, on trace A. This picture was read for more than 10 minutes and was deteriorated by positive ion landing to the potential shown on trace B. ELID was applied by flooding with electrons from a cathode which was set to about -25 volts with respect to the base of the target. Trace C shows the signal after enhancing for a few seconds. Here the

* The basic principles of ELID were presented before the IRIS in May of 1962 in a paper by Dr. A.S. Jensen and M.P. Siedband.

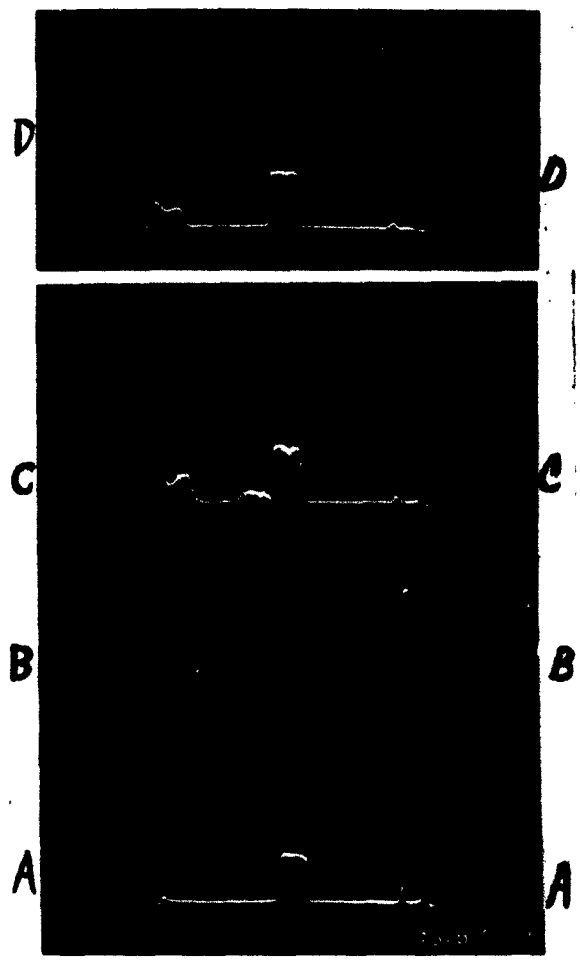


Figure 13. Signal Track on A-Scope for ELID

signal had been multiplied by about 2.5. The picture was then deteriorated to about the level of trace B, whereupon it was again intensified, resulting in the potentials shown on trace D. The enhancement was so powerful that the noise on trace C was pushed outside the latitude of the transfer curve as shown in trace D. Many such experiments have been made and several had an enhancement of 20 times.

In the following description, it is shown how ELID can be derived from the secondary emission curve of the target dielectric. For clarity, charge potentials with respect to the target base were arbitrarily chosen to be -1 to -5 volts. A signal enhancement of 2 times was assumed.

Figure 14 shows the negative dielectric charge A to E with respect to the target base. Figure 15 shows the potentials of these points plotted against their positions

on the target. The slope of this curve thus is a measure of contrast. Figure 16 is a representative secondary emission ratio curve for a storage dielectric with a first crossover at 25 volts. The potentials of A to E are shown on the curve as they are seen from the cathode. Figure 17, which is derived from figure 16, shows the number of electrons landing per second on the target surface (primary minus secondary). Spots A to E are again shown in their positions on the curve. In B, twice the number of electrons land as in A; in C, three times; in D, four times; and in E, five times as many.

After flooding for a short time, the conditions shown in figure 18 are reached where all points have received a charge which is linearly proportional to their previous charges. As shown in figure 19, the potentials of the points A to E (now A' to E') with respect to the target base have doubled. The slope of $\gamma'$ is twice the slope of $\gamma$ on figure 15. Therefore the contrast has effectively been doubled. This signal enhancement process can be repeated a number of times.

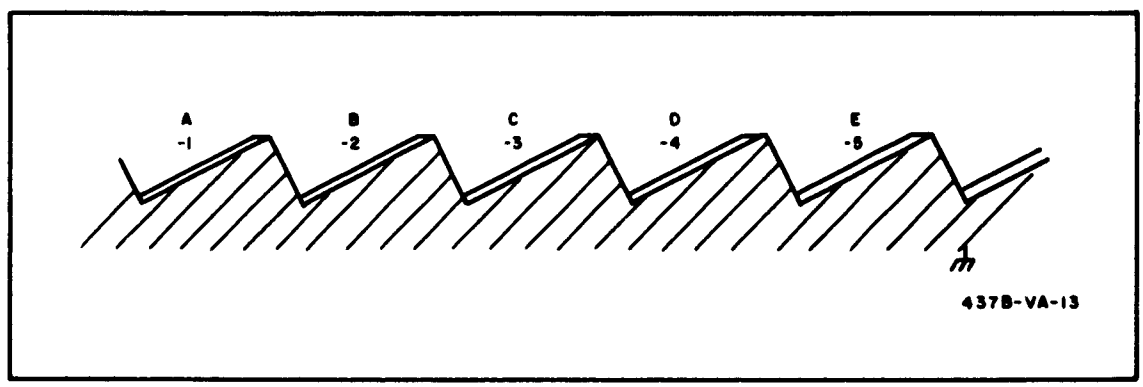


Figure 14. Negative Dielectric Charge
Referred to the Target Base

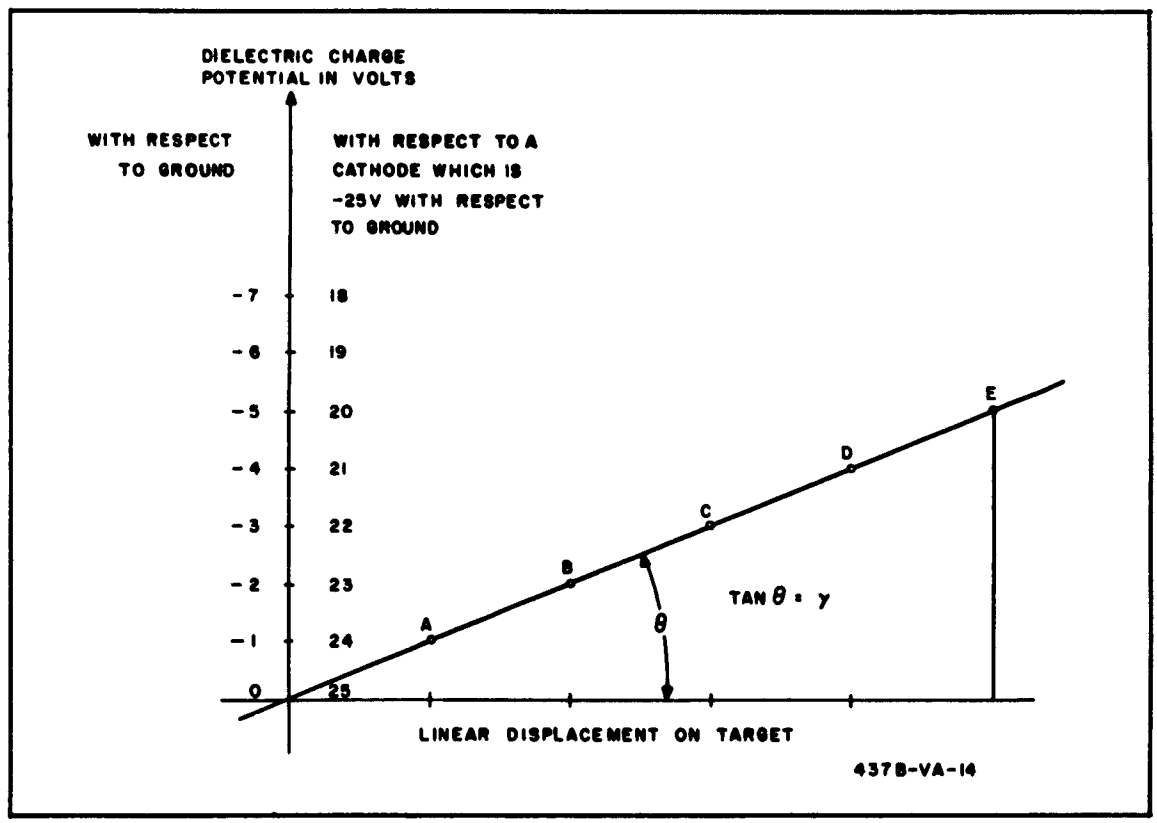


Figure 15. Point Potential vs Position on Target

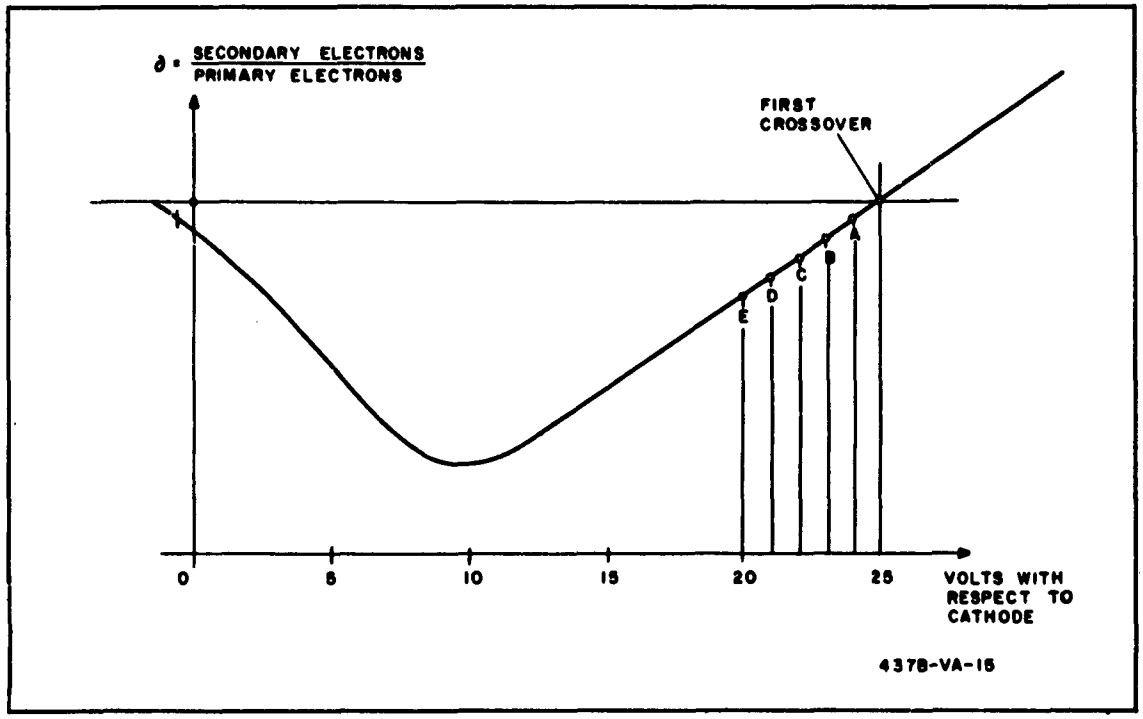


Figure 16. Secondary Emission Ratio

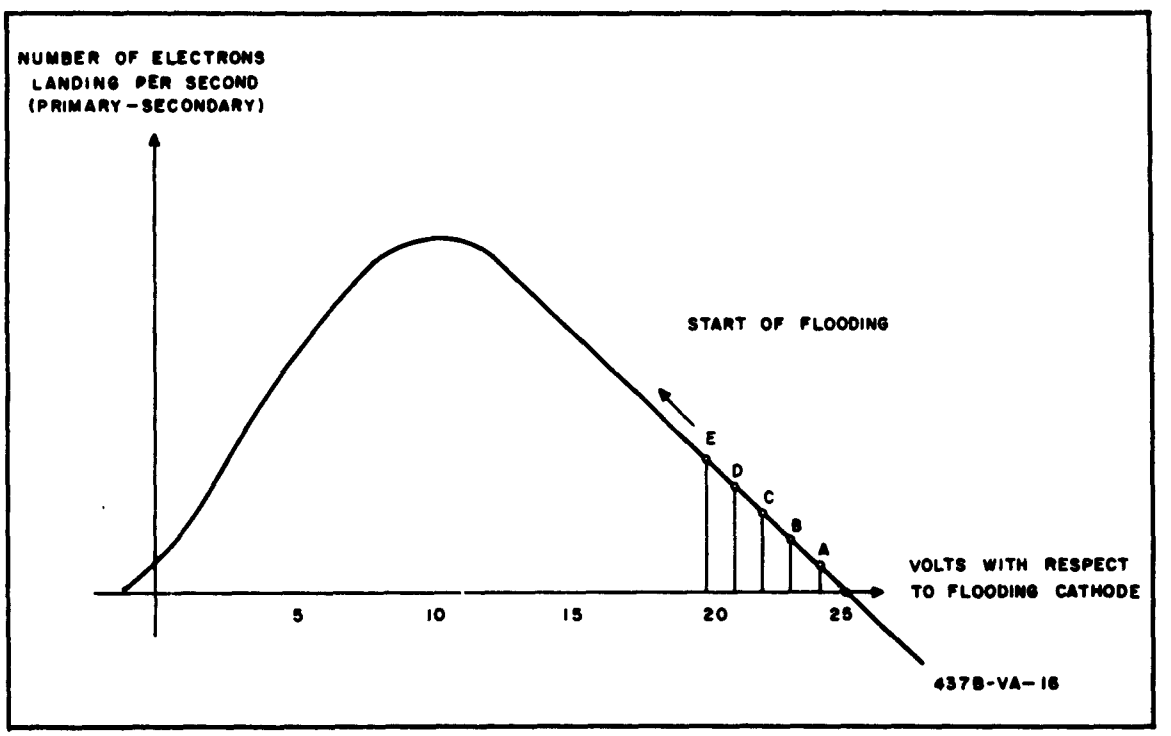


Figure 17. Electron Flux

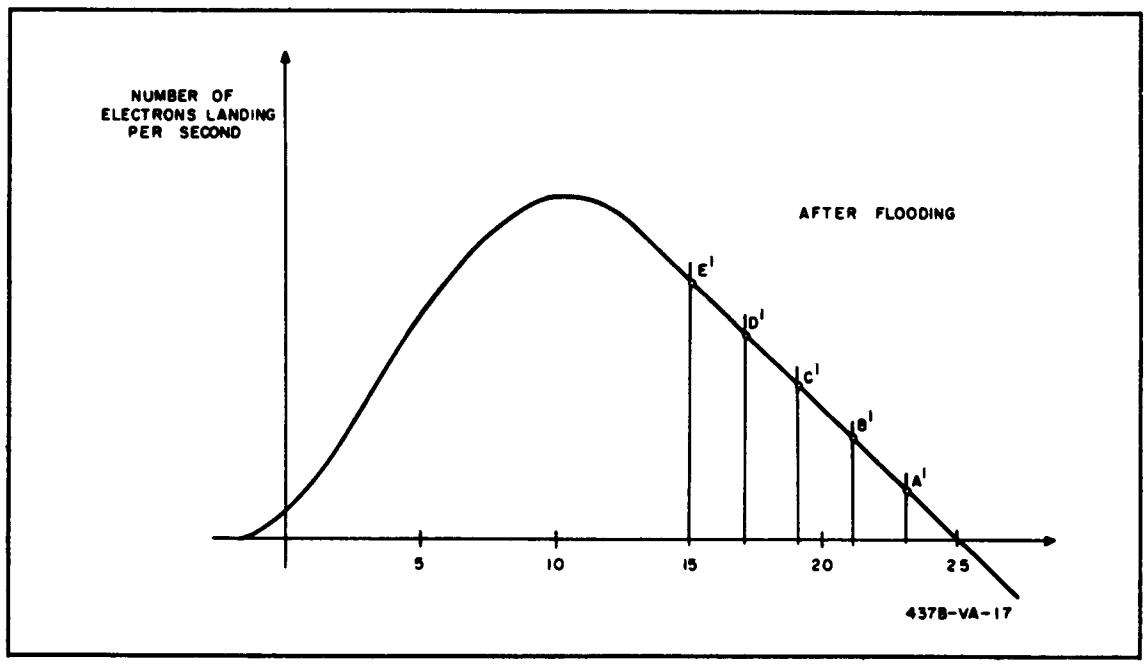


Figure 18. Results of Flooding

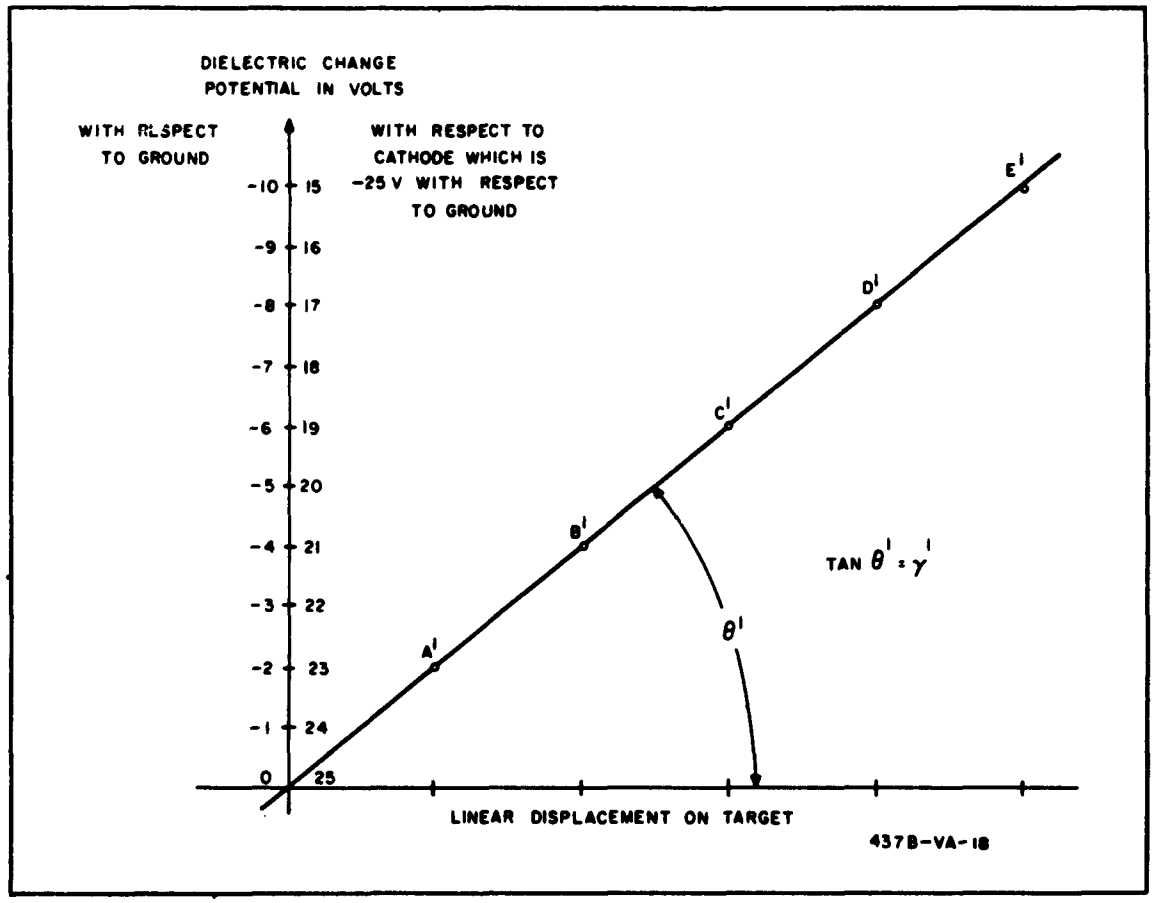


Figure 19. Point Potential vs Position on Target

# 3. PROGRAM FOR NEXT INTERVAL

## 3.1 DEMOUNTABLE VACUUM SYSTEM

In the demountable ultraviolet system, the storage and readout characteristics of continuous layer dielectric targets will be compared with the normal grooved ones. Polystyrene dielectrics will be used on both smooth and grooved targets to measure electrical capacity and writing speed. Several new shaved cathodes on passive nickel are ready for use in the demountable system. Resolution measurements will be compared with previous ones.

## 3.2 SPIRAL ACCELERATOR

Spiral accelerators will be fabricated for use in photodiodes and in flip target tubes.

## 3.3 STORAGE TARGET

Blemish-free masters from optical gratings will be made in an electrolytic bath which will be installed in one of the clean rooms that has been made available for it. From these masters, blemish-free replicas for the flip target tubes and the demountable system will be made.

Replicas will be made from 1000-line gratings. Also compound target plates with 1000-, 2000-, 4000-, and 6000-groove parts will be electroformed for use in flip target tubes. These target plates will be used in measuring the resolution disturbances introduced by the grooves. Methods of cleaning targets before the dielectric evaporation and before their assembly in tubes will also be studied.

Correlating the curves of figure 9 will be continued by measuring readout transfer curves on more targets and by taking into account the contact potentials and the thermal spread of the beam electrons.

## 3.4 ELECTRONIC EQUIPMENT

Every effort will be made to reduce further the 60-cycle interference in the slow scan unit. Also if a higher resolution can be gained, the unit may be combined with the electron writing on photographic emulsions.

The 4.5-inch deflection yoke with focus and alignment coils will be installed on the cradle for the 4.5-inch flip target tube. The measurements for the additional focus coil and the fabrication of it will be finished. This new unit will be energized from the power supply of the slow scan device.

## 3.5 VACUUM TUBE DEVELOPMENT

Several slit target tubes with the new reading cathodes will be built and beam size measurements will be performed.

Monoscopes with 1000-groove-per-inch targets will be used with a magnetic field which will change the angle of incidence of the electrons, thereby permitting beam size to be measured. The monoscope conductors on both the long and short grooves will have dissimilar secondary emission curves. The monoscope targets will have 1000-line gratings in the X- and Y-directions for measuring astigmatism in the beam. For additional beam measurements, monoscopes with targets having Westinghouse Diminishing Bar Resolution Patterns etched in the X- and Y-directions will be assembled. These resolution patterns will contain as few as 3000 TV lines per inch.

Additional measurements will be made of the spectral response of bialkali photodiodes.

The uniformity of the photodiode photocathodes will be measured by precise cross-movements of the diodes behind a 1/8-inch hole. Response curves will be plotted over a 2.25- by 2.25-inch field. Aperture response will be measured on the diodes with the aid of optics having a calibrated axial beam. The Westinghouse bar pattern will be projected near the lens axis, and the photodiode will be moved across it. Aperture response versus the distance from the photocathode center will be plotted.

Measurements of the secondary emission target capacity and EBIC and ELID gain will be refined and continued.

## 3.6 OVERALL PERFORMANCE OF THE TVIST SYSTEM

The optimum aperture response curve of the whole system will be determined for a 4.5-inch flip-over target tube. This optimum response will be a combination of the optics, the electron optics of the image section, the writing resolution, the groove disturbance (if any), the reading beam resolution, and the amplifier and recording resolution. Plots of resolution versus contrast and resolution versus exposure energy will be obtained.

# APPENDIX A

## STUDY OF DIELECTRICS

To facilitate selecting compounds having high specific resistance and low dielectric constants, it is desirable to compare the existing data on the dielectric constants and specific resistances of the various alkali and alkaline-earth halides and oxides which can be used in vacuum evaporation thin film studies. A desirable minimum for the volume resistivity, $\rho$, would be on the order of $10^{18}$ ohm-cm. Other desirable qualities include good evaporation characteristics and the capability of good adhesion to the substrate.

The dielectric constant, $\epsilon$, of an insulator is the ratio of the parallel capacitance, Cp, of a given set of electrodes with the material being studied as the dielectric to the capacitance, Cr, of the same electrode configuration with a vacuum as the dielectric. Methods of measuring $\epsilon$ are best described in ASTM Standards, Part II; 1961; p. 859-912.

Electrical resistance, in particular volume resistivity $\rho$, is calculated from the formula

$$\rho = AR_{v/s}$$

where

$R_v$ = volume resistance, in ohms

s = average thickness of sample

A = effective area of the electrodes

For approved methods of measurement refer to ASTM Standards Part II, 1961; pp. 988-999.

Generally speaking, a strong and rigid chemical bond in an oxide or halide will produce high resistivity and a small dielectric constant. This characteristic is also to be expected in a good insulator, according to E. Ryshkewitch[1]. One simple means of relating chemical bonding to electric properties is through a study of lattice energies.* According to an article by A. P. Nakhodnova[2], the electrical conductivity,

* Lattice energy is the energy required to separate the ions of a crystal to an infinite distance from each other.

dielectric constant, and tan δ generally all increase as the lattice energy decreases. For example, note the relationships between the lattice energy and the dielectric constants of various alkaline-earth oxides in the table below. The lattice energy is given in kilocalories per mole.

| Compound | BeO | MgO | CaO | SrO | BaO |
|---|---|---|---|---|---|
| Lattice energy[3] | 1080 | 936 | 830 | 784 | 740 |
| Dielectric constant[4] $\epsilon$ | 7.35 | 9.65 | 11.8 | 13.3 | 34.0 |

Unfortunately, no published data were available at the time of this report to correlate the hypothesis with the fluoride group, but there is no reason to believe that the pattern is not the same. Thus it has become possible to select a low dielectric constant compound from other groups in the periodic chart when the data are available.

A comparison of the negative heat of formation energy* ($-\Delta F_f$) of the compound with its dielectric constant indicates the periodicity shown in the following tables. The negative heats of formation are given in kilocalories per mole.

| | LiF | NaF | KF | RbF | CsF |
|---|---|---|---|---|---|
| $\epsilon$[1] | 9.27 | 6.00 | 6.05 | 5.91 | 5.90 |
| $-\Delta F_f$[5] | 145.6 | 136 | 134.5 | 133.2 | 126.9 |

| | $BeF_2$ | $MgF_2$ | $CaF_2$ | $SrF_2$ | $BaF_2$ |
|---|---|---|---|---|---|
| $\epsilon$[1] | <5.0 | 5.30 | 6.76 | 7.69 | 7.33 |
| $-\Delta F_f$[5] | 251.4 | 263.5 | 290.3 | 289.0 | 286 |

It appears that $BeF_2$ and the alkali halides and fluorides most nearly approach the requirements of a low dielectric constant. Although their specific resistances are not presently known, it must be assumed that they are very high since all of these compounds have high chemical bonding strengths.

* Formation energy is the negative heat energy of formation of the compounds from the elements.

The dielectric constants of the alkaline earth and alkali salts exhibit predictable trends according to their position in the periodic table with respect to ascending or descending atomic number. Exceptions are the fluorides and chlorides of lithium which have inordinately high dielectric constants. The exceptions probably occur because lithium salts deviate from the structure of the others in Group Ia of the periodic table. Note that in the alkaline earth group, the tendency is for the dielectric constant to increase with the increase in atomic number. However, the more electropositive ion ($Be^{++}$) has a low dielectric constant while in the Group Ia series, three of the alkalis have approximately the same value. This condition is probably explained by the fact that the crystal lattices of Na, K, Rb, and Cs salts are all cubic, while those of Li, Ba, Sr, Ca, and Mg are more complex and have entirely different lattice energies. In general, those salts with the most compact and stable cubic structure offer the best possibilities for low dielectric constant and high resistance.

Investigation of the resistivities and dielectric constants of the oxides and halides of the various atomic groups in the periodic table shows the choice of inorganic salts to be rather limited. Further investigation of the Group Ia and Group IIa salts shows that only a few chlorides and fluorides have good insulation properties and are suitable for vacuum evaporation. The chlorides are those of Na, K, Rb, and Cs and the fluorides are those of Be and Mg.

The only other suitable compounds might come from the oxides of groups IIIa, IVb, Vb, and VIb. However, the evaporation characteristics of those compounds with the lowest dielectric constants are not good, and other means must be used to obtain them in thin films with good strength and high density. Also the oxides from these groups are particularly susceptible to poisoning by other elements, including common gases. The resistivities of these oxides decrease very rapidly with only a small contamination. In addition, it is extremely difficult to process these materials into their theoretically maximum density, purity, and resistance states. Ryshkewitch[1] gives a rather thorough treatment of the oxides of Al, Mg, Be, Ca and a few of the rare earths. The sampling of the resistivities and dielectric constants of the transitional oxides given below shows that generally they do not meet the requirements of the problem[1]. (See also figures A-1 and A-2.)

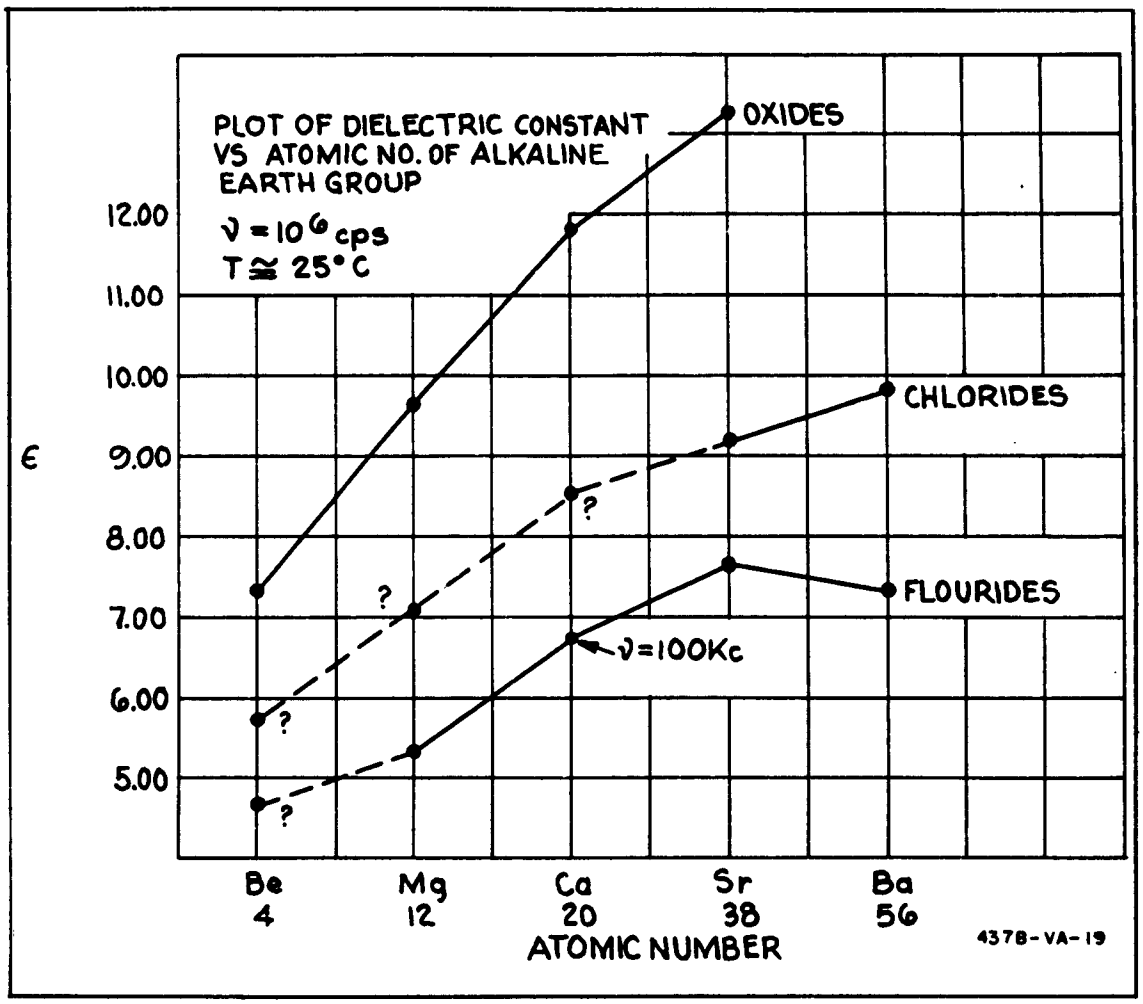


Figure A-1. Dielectric Properties of Metal Salts

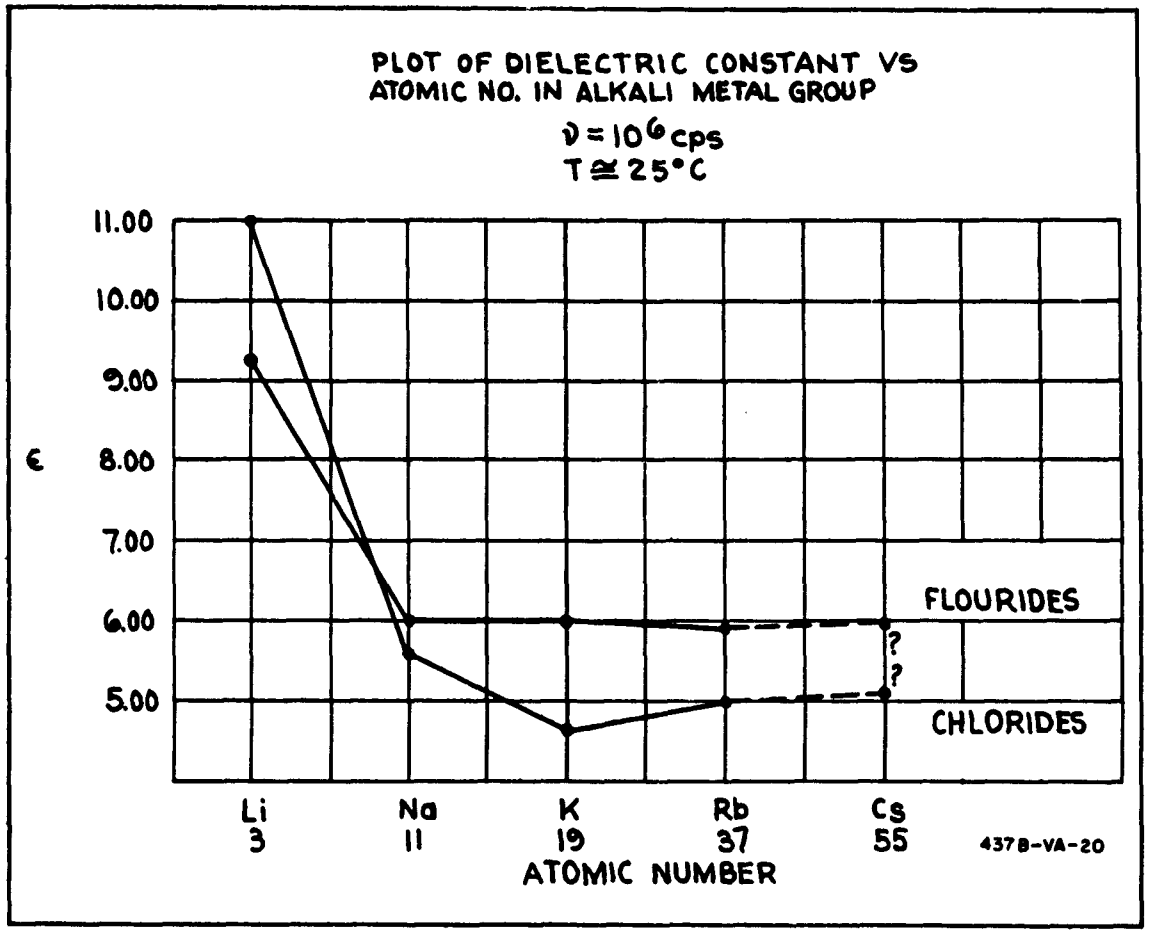


Figure A-2. Dielectric Properties of Metal Salts

| Oxide | Dielectric Constant | Specific Resistance |
|---|---|---|
| $Ta_2O_5$ | 11.6 | |
| $TiO_2$ (Rutile) | 100.0 | |
| $Cr_2O_3$ | 12.0 | |
| $ZrO_2$ | 12.5 | 3300 ohm-cm (697°C) |
| $Ba_2SiO_4$ | 13.0 (theoretical) | |
| $CeO_2$ (Ceria) | 7.0 | $5 \times 10^7$ ohm-cm (500°C) |
| BeO | 6.3 (Bur. of Stds) | $10^8$ ohm-cm (500°C) |
| $Al_2O_3$ (High Dens) | 9.39 | $1.2 \times 10^{13}$ ohm-cm (300°C) |

Mention might be made of the work by Hass, Ramsey and Thun[6] on some of the rare earth oxides and fluorides used for evaporated films. Although the authors give no data for resistivity and dielectric constant, they do reach the following conclusions:

a. The oxides are usually condensed as nearly amphorous films.

b. The fluorides are usually condensed as large grains.

c. All films are hard and have excellent chemical and mechanical durability.

d. Amphorous film structures frequently are more influenced by small changes in deposition condition than are the well crystallized forms.

This information, too, indicates that the fluorides and chlorides of Groups Ia and IIa are probably the best choices for vacuum evaporated films unless a choice can be made from such organic materials as polyethylene[7] (dielectric constant = 2.3 and resistivity = $10^7$ to $10^9$ ohm-cm), polystyrene[7] (dielectric constant = 2.7 and resistivity = $10^{17}$ to $10^{19}$ ohm-cm), or teflon[9] (dielectric constant $\approx$ 2.0 and resistivity $>10^{15}$ ohm-cm).

# BIBLIOGRAPHY


1. Ryshkewitch, E., Oxide Ceramics, Academic Press, New York, 1960.

2. Nakhodnova, A. P., Izvest. Tomsk, Politekh. Inst., 91, (1956), 209-218.

3. Remy, H., "Treatise on Inorganic Chemistry," Vol. I, Elsevier Publishing Company, Amsterdam, (1956), 235.

4. American Institute of Physics Handbook, McGraw-Hill Book Company, New York, (1957), 5-115.

5. Hadley, Kramer, and Royce, JOAP, 27, 11, (November 1956), 1384-1385.

6. Hass, Ramsey, and Thun, "Optical Properties of Fluorides," JOSA, 49, 2, (February 1959), 116-120.

7. "Table of Properties," Plastic Catalog, Kaufman Glass Co., Wilmington, Delaware.

8. "Teflon FEP - Fluocarbon Film," du Pont Report, Wilmington, Delaware. (April 1959).